

Are Medium Modifications of the Nucleon Structure Suggested by a Chiral Quark-Meson Theory Reliable?

Christo V. Christov^{1,2}

¹Institut für Theoretische Physik II, Ruhr-Universität Bochum, Germany

²Institute for Nuclear Research and Nuclear Energy,
Bulgarian Academy of Sciences, Sofia 1784, Bulgaria

Abstract. In this contribution the medium modifications of the nucleon structure in a dense matter, suggested by a chiral quark-meson theory, are discussed in regard to both quasi elastic (QES) and deep inelastic scattering (DIS) data. In the theory a hybrid NJL model is used in which a Dirac sea of quarks is combined with a Fermi sea of nucleons. The mesons are described as collective $\bar{q}q$ excitations and the nucleon appears as a baryon-number-one soliton of N_c valence quarks coupled to both Dirac and Fermi sea. If the medium density reaches nuclear matter one, the proton radius shows an increase of 19% and the nucleon mass a decrease of 17%. The magnetic moments and axial vector coupling constant are less modified. All form factors show remarkable reduction at finite transfer momenta. The predicted medium modifications are examined in the analyses of experimental data of QES and DIS. In the case of QES the use of the medium modified nucleon form factors within CDFM model improves considerably the comparison with the experimental data for the longitudinal response function. In the case of DIS the medium modified values, in particular the nucleon mass and radius, are consistent with values used in different models considering the EMC-effect.

1 Introduction

Over more than 40 years the Quantum chromodynamics (QCD) has been established and generally accepted as the theory of strong interaction which has to describe the structure and the dynamics of hadrons. Quarks and gluons are the elementary constituents of QCD and at very high-energies quarks and gluons interact very weakly (Asymptotic freedom). The prominent feature is that at low-energies QCD has a strong non-perturbative nature which is characterized by the confinement – the force between quarks strongly increases as they are separated and by the dynamical chiral symmetry breaking leading to a constituent quark mass.

The two main challenges of QCD still remain open. From one side it is the description of the hadron structure and dynamics. From the other side it is QCD thermodynamics, in particular the QCD phase diagram.

From the side of the experiment the the hadron structure is widely studied and there are a lot of experimental data available. A special interest is devoted to the quasi-elastic electron scattering (QES) and deep-inelastic lepton scattering (DIS) since both allow for probing the nucleon properties immersed in the nucleus. In contrast to the hadron structure QCD phase diagram is experimentally almost not studied. However there is an increasing interest and many experiments have been planned (see Figure 1).

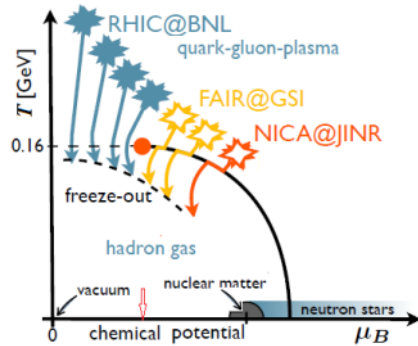


Figure 1. Generally expected phase-diagram of QCD for nuclear matter. The solid lines show the phase boundaries for different phases. The red solid circle corresponds to the estimated critical point. The areas reached at different accelerator facilities are also shown [1].

Despite of the progress done from the side of the theory so far, the lattice QCD is still not developed enough to allow the solution of low-energy non-perturbative phenomena, especially if nucleons are involved. It is a motivation to apply for this effective quark-meson models which incorporate at least one of the main features of the low-energy QCD, namely confinement or dynamical chiral symmetry breaking.

In particular the models based on the Nambu-Jona-Lasinio (NJL) Lagrangian are very popular since they incorporate the chiral symmetry breaking and describe properly the meson sector. Since NJL model [2] has the same flavor symmetries as QCD, it can be interpreted as a low-energy chiral effective theory of QCD (see for instance Kahana and Ripka [3], Dyakonov and Petrov [4] ...) considering $1/N_c$ ($N_c \approx 3$) as a small parameter (t'Hooft [5]) in which the non-local vertex is replaced by a local one (see Figure 2).

Since the NJL model lacks confinement its applicability is restricted to low-energy region.

It was the motivation to apply a chiral quark-meson model (see for review [7] and references therein) for these analyses. The model is able to reproduce quite reasonably the nucleon and delta properties as well as the corresponding form factors of the free nucleon. Within the model the free nucleon is considered as

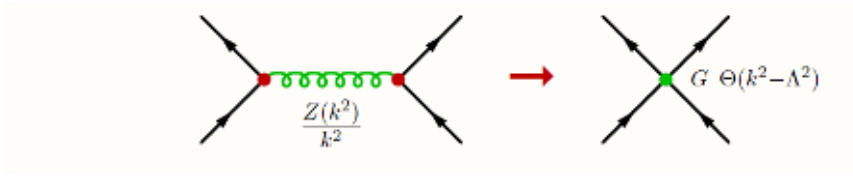


Figure 2. QCD non-local interaction vertex reduced to NJL local one.

a localized bound state of N_c quarks coupled to the polarized Dirac sea. The mean-field approximation is used, which means that the meson quantum (loop) effects are not considered. In order to consider the medium effects on the nucleon structure in the model a Fermi sea is added. The model has been applied to study the QCD thermodynamic bulk properties as well [8].

2 Chiral Quark-Soliton Model

The chiral quark-soliton model (for details see review [7] and references therein) is based on the SU(2)-version of the NJL Lagrangian [2] which contains chirally invariant local scalar and pseudoscalar four-quark interaction:

$$\mathcal{L} = \bar{\Psi}(i \not{\partial} - m_0) \Psi + \frac{1}{2} G [(\bar{\Psi} \Psi)^2 + (\bar{\Psi} i \boldsymbol{\tau} \gamma_5 \Psi)^2], \quad (1)$$

where Ψ is the quark field, G is the coupling constant, $\boldsymbol{\tau}$ are the Pauli matrices in the isospin space and m_0 is the current quark mass taken equal for both up and down quarks. Applying the well-known bosonization procedure the NJL Lagrangian is expressed in terms of the auxiliary meson fields σ, π :

$$\mathcal{L} = \bar{\Psi}(i \not{\partial} - \sigma - i \boldsymbol{\pi} \cdot \boldsymbol{\tau} \gamma_5) \Psi - \frac{1}{2G} (\sigma^2 + \boldsymbol{\pi}^2) + \frac{m_0}{G} \sigma, \quad (2)$$

Pions play the role of Goldstone bosons. Because of the small current quark mass m_0 (some MeV) the chiral symmetry is explicitly broken and pion are not massless ($m_\pi \approx 140$ MeV). Through the dynamically broken chiral symmetry the quarks acquire a constituent mass M of some hundred MeV.

Due to the local four-fermion interaction the lagrangian (1) is not renormalizable and a regularization procedure with an appropriate cut-off Λ is needed to make the effective action finite:

$$\text{Tr} \ln \hat{A} \rightarrow -\text{Tr} \int_{\Lambda^{-2}}^{\infty} \frac{ds}{s} e^{-s \hat{A}}. \quad (3)$$

The cut-off parameter Λ is taken big enough not to influence the model results. Actually only the part of the effective action coming from the Dirac sea (negative-energy part of the spectrum) is divergent and it needs to be regularized.

The parameters of the model, namely the current mass m_0 , the cutoff Λ and the coupling constant G . In the vacuum sector, m_0 is fixed reproducing the

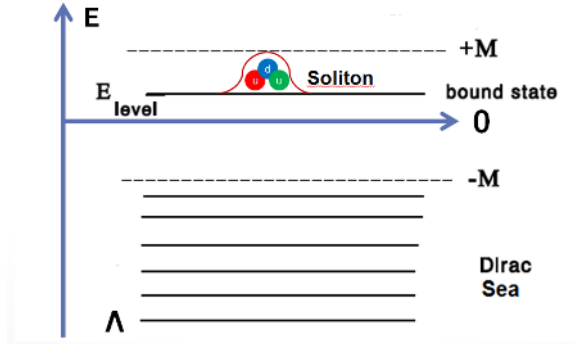


Figure 3. The bound state of N_c valence quarks coupled to the polarized Dirac sea.

physical pion mass $m_\pi = 140$ MeV and the pion decay constant $f_\pi = 93$ MeV. It leads to the well-known Goldberger-Treiman (GT) relation on the quark level

$$M_0 = g_\pi f_\pi . \quad (4)$$

and one also recovers the Gell-Mann-Oakes-Renner (GMOR) relation.

The only free parameter remained is the constituent quark mass $M_0 = 420$ MeV is taken to reproduce properly the properties of a free nucleon (see [7] and references therein). The corresponding value of the proper-time cutoff used is $\Lambda = 640$ MeV. The value is taken large enough not to influence to results.

In the chiral quark-soliton model the nucleon is a projected non-topological $B = 1$ soliton. It is treated as a bound state of N_c valence quarks coupled to the polarized Dirac sea (Figure 3) [7]. The soliton is a localized mean-field (hedgehog) solution (large N_c approximation), which means that the meson quantum (loop) effects are not included. Solving the corresponding equations of motion in an interactive self-consistent procedure this solution is found.

Since the hedgehog soliton does not preserve the spin and isospin, in order to get the nucleon states with proper spin and isospin one has to quantize the soliton, making use of the rotational zero modes in the leading order in $1/N_c$ (see Figure 4).

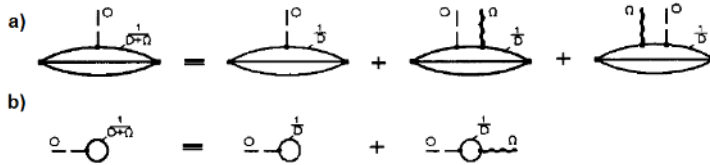


Figure 4. Diagrams of expansion in Ω : a) valence contribution; b) Dirac sea contribution.

As can be seen from [7] and references therein the chiral quark-soliton model reproduces the properties of the free nucleon rather well.

3 Nucleon as a Non-Topological $B = 1$ Soliton in the Medium

The nucleon in a medium appears as $B = 1$ localized bound solution (soliton) of N_c valence quarks interacting with the Fermi and Dirac sea both getting polarized due to the interaction (Figure 5) [10–12]. In the picture the mesons appear as $\hat{q}q$ excitations but they are also directly coupled to the Fermi sea as well.

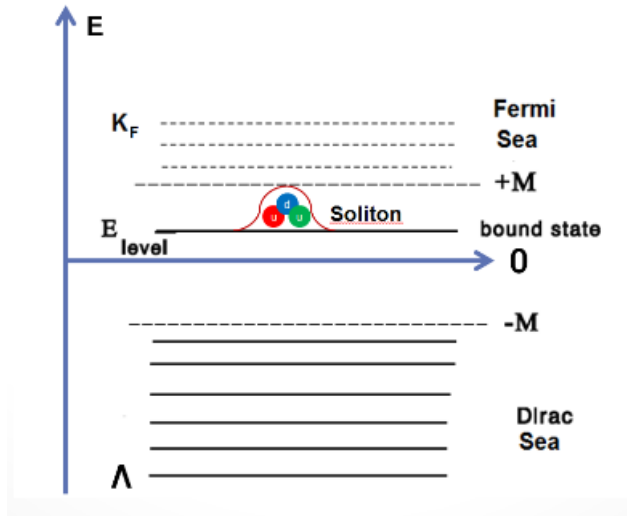


Figure 5. The bound state of N_c valence quarks coupled to the polarized Dirac sea.

Since the Fermi sea contribution is finite it is not regularized.

The soliton solution has to be projected in order to get proper spin and isospin numbers [11, 12]. It is done in $1/N_c$ expansion up to leading order (see Figure 4). A variational procedure based on mean-field states of a generalized hedgehog structure and spin- and isospin-projection is employed. Details are presented in [12].

The numerical results concerning the static nucleon properties at finite medium density are summarized in Table 1.

The calculated square radii presented in Table 1 show a similar behaviour (bound to increase) except that of the neutron charge radius which is reduced. Thus our numbers show a “swelling” for the proton charge distribution and a “shrinking” for the neutron one. Since most of the observables are dominated up to 70% by the quark contributions the swelling of the quark fields causes an increase of the total radii. It is not the case of the neutron charge radius where the negative pion tail, which dominates at large distances, is responsible for the

Table 1. Medium effects on nucleon properties. The medium values of the meson sector are given together with the observables and square radii of the nucleon in dependence on the medium density ρ_B . For finite medium densities the values are given relative to the theoretical numbers at $\rho_B = 0$

Quantity	Absolute values		Relative values	
	Experiment	$\rho_B = 0$	$\rho_B = \frac{1}{3}\rho_{nm}$	$\rho_B = \rho_{nm}$
f_π (MeV)	93	93	0.89	0.77
m_π (MeV)	139.6	139.6	1.06	1.14
m_σ (MeV)		937.7	0.93	0.85
E_N (MeV)	938	938	0.92	0.83
$E_\Delta - E_N$ (MeV)	295	156	0.92	0.79
$\langle r_c^2 \rangle_p$ (fm ²)	0.74	0.662	1.21	1.41
$\langle r_c^2 \rangle_n$ (fm ²)	-0.12	-0.094	0.92	0.80
$\langle r_m^2 \rangle_p$ (fm ²)	0.706	0.765	1.11	1.28
$\langle r_m^2 \rangle_n$ (fm ²)	0.757	0.802	1.10	1.25
$\langle r_A^2 \rangle$ (fm ²)	0.507	0.4775	1.19	1.48
μ_p (n.m.)	2.79	2.82	1.05	1.11
μ_n (n.m.)	-1.91	-2.44	1.03	1.07
g_A	1.23	1.77	0.97	0.94
$g_{\pi NN}$	13.6	17.1	1.00	1.00

negative sign of the neutron square charge radius at zero density. Since at finite density the magnitude of the pion field gets reduced and the quark charge distribution show a swelling the neutron square charge radius becomes less negative.

Our results for the magnetic moments, the axial vector coupling constant g_A and pion-nucleon coupling constant $g_{\pi NN}$ are also presented in Table 1. It should be mentioned that the quantity denoted as magnetic moment in the medium is defined as $G_M^*(q^2 = 0)/2M_N^*$, since this combination appears in the Rosenbluth formula. In contrast to the radii the g_A and the magnetic moments are less affected by the medium. For the proton magnetic moment a tendency to increase can be concluded whereas for the neutron such a clear trend cannot be concluded. The g_A decreases slightly – at ρ_{nm} the reduction is about 6%. This change is rather small to explain the quenching of 20% suggested for this quantity in nuclei from the analyses of beta decay data. The pion-nucleon coupling constant is the only quantity practically not affected by the medium.

The calculated form factors are shown in Figures 6–11. The experimental data [16] depicted correspond to the vanishing medium density.

At finite momentum transfers ($q^2 \geq 0.15$ GeV) the form factors show a clear trend to decrease with growing medium density. With increasing momentum transfers they get relatively more reduced. Their slope at the origin, except for the electric form factors, increases and it is reflected in the medium values of the corresponding mean square radii.

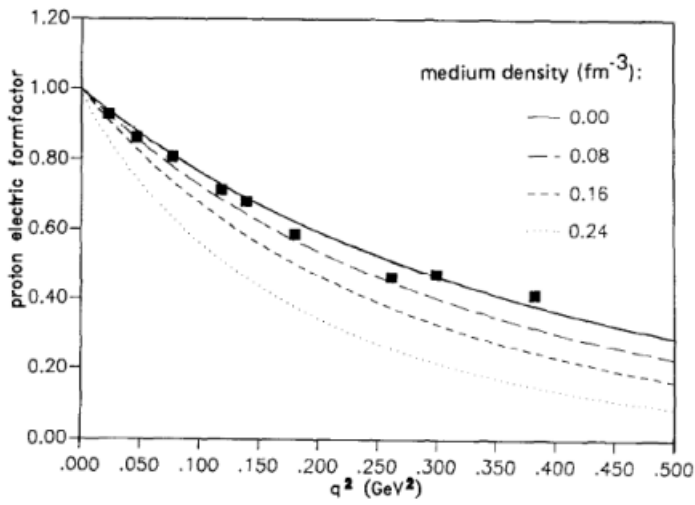


Figure 6. Proton electric form factor plotted versus q^2 for various baryon densities of the medium. Experimental data are from [16].

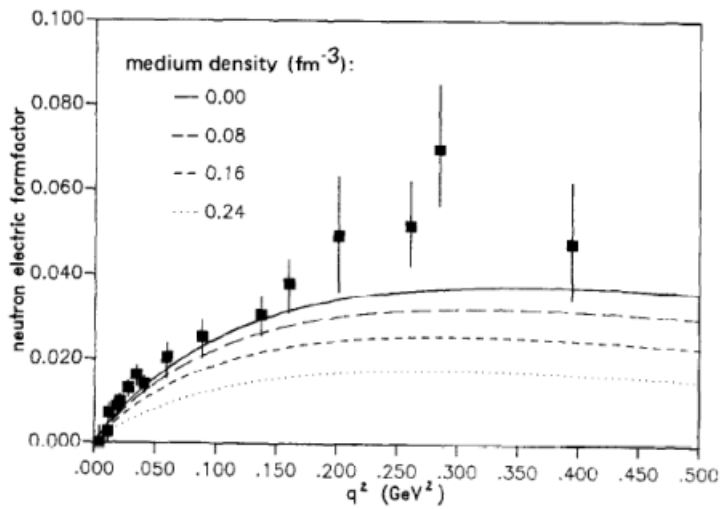


Figure 7. Neutron electric form factor plotted versus q^2 for various baryon densities of the medium. Experimental data are from [13].

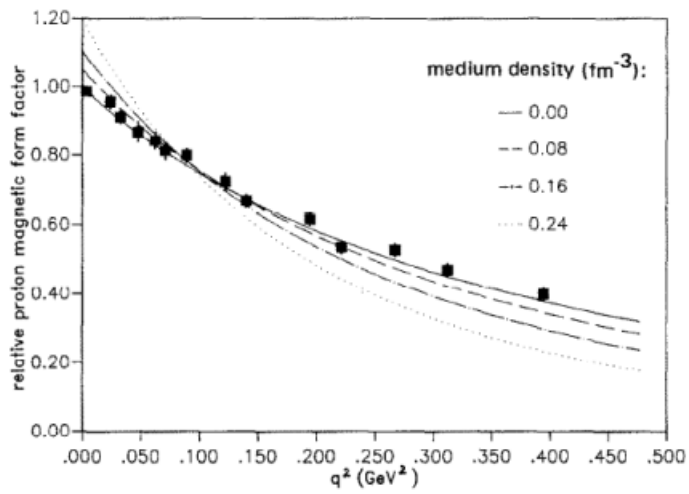


Figure 8. Proton magnetic form factor plotted versus q^2 for various baryon densities of the medium. Experimental data are from [13, 14].

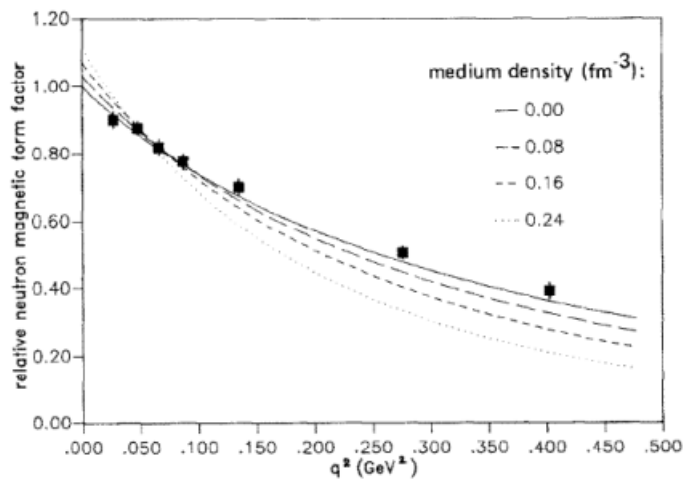


Figure 9. Neutron magnetic form factor plotted versus q^2 for various baryon densities of the medium. Experimental data are from [13].

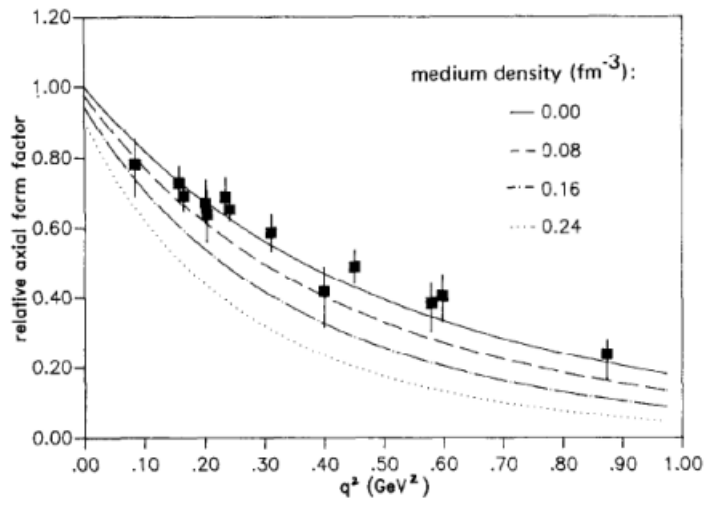


Figure 10. Axial form factor $G_A(q^2)/g_A$ plotted versus q^2 for various baryon densities of the medium. Experimental data are from [14].

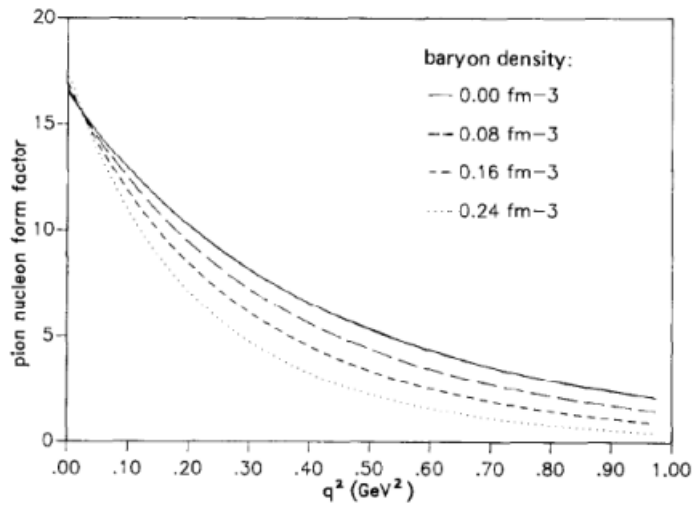


Figure 11. Pion nucleon form factor $G_A(q^2)/g_A$ plotted versus q^2 for various baryon densities of the medium.

Although the pion nucleon coupling constant is not affected by the medium the corresponding form factor at finite momentum transfers also decreases with growing medium density. To be consistent one should taken into account this behavior of $G_{\pi NN}$ in the construction of the NN potential (especially its isovector tensor part) for description of the N -nucleus scattering or in charge-exchange reactions.

4 Medium Modified Nucleon Properties in Analyses of Quasielastic Electron Scattering (QES) and Deep Inelastic Scattering Data

4.1 Medium modified nucleon properties in analyses of QES

Since the longitudinal response function of QES is proportional to the squared electric form factor, it allows for a direct check of the right order of magnitude of the medium effects.

Using the Coherent density fluctuation model (CDFM) [15] the longitudinal response function as well as the Coulomb sum rules for the quasielastic electron scattering are calculated for wide range of momentum transfers and various nuclei with medium-modified effective masses and form factors. Results for the longitudinal response function are presented on Figure 12.

The results presented are calculated using different nuclear models. Even in the case of Fermi-Gas Model there is a significant improvement of the comparison with the experimental data. It is a strong indication that the medium effects play a decisive role and not the nuclear structure.

In contrast to the longitudinal channel the transverse response is affected by meson exchange currents and delta electroproduction. Since both contributions are ignored in the present approach it is not surprising that we have problems in reproducing the experimental data at higher energy transfer. This makes the transverse response inappropriate as a signature for the "swelling" of the nucleon. Actually we expect this channel to be more sensitive to the single-particle structure than the longitudinal one because the magnetic transitions, dominant in this channel, are strongly spin dependent. It is confirmed by the comparison of the shell-model calculations with the those of the Fermi-Gas model.

Coulomb sum rule is defined as an integral over the energy transfer (at constant three-momentum transfer q) of the longitudinal response, normalised to the charge of the nucleus and the electric form factor of the free proton

$$C(q) = \int_{\omega_{el}}^{\omega_{max}} \frac{R_L(q, \omega)}{ZG_E^p{}^2} d\omega .$$
 The results are presented on Figure 13.

As can be seen from Figure 13 for all nuclei considered, the incorporation of medium effects on the nucleon mass and form factors even in the FGM seems to remove the discrepancy between theory and experiment in a plausible way.

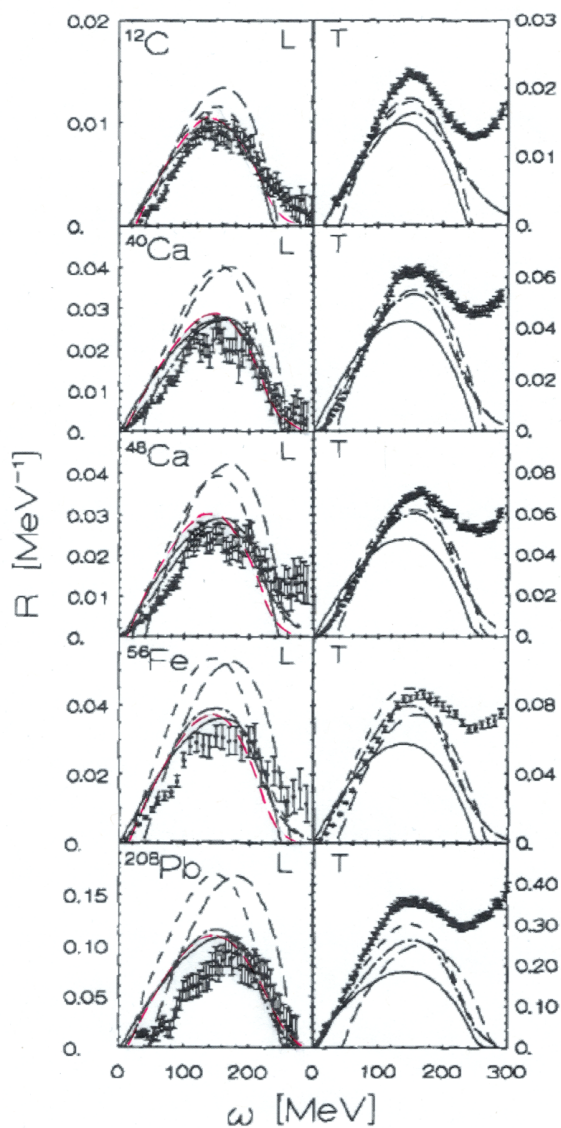


Figure 12. Longitudinal and transverse response functions for ^{12}C , ^{40}Ca , ^{48}Ca , ^{56}Fe and ^{208}Pb at 500 MeV/c momentum transfer: red-dashed line: CDFM with medium modification of nucleon properties; short-dashed (dash-dotted) line: shell-model calculations without (with) medium modifications of nucleon properties; long-dashed (solid) line: FGM results without (with) medium-modified nucleon properties. Experimental data are from [16].

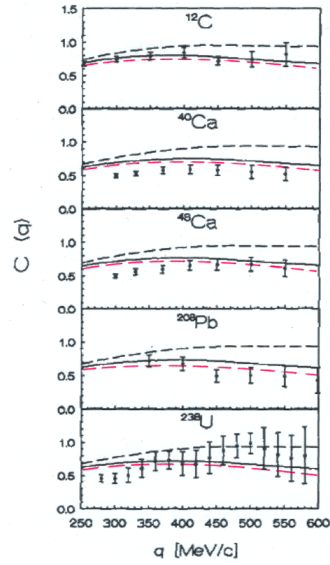


Figure 13. Coulomb sum rule for for ^{12}C , ^{40}Ca , ^{48}Ca , ^{56}Fe , ^{208}Pb and ^{238}U : red-dashed line: CDFM with medium modification of nucleon properties; dashed (solid) line – FGM results without (with) medium-modified nucleon properties. Experimental data are from [16].

4.2 Medium modified nucleon properties in analyses of DIS data

The general expectation was that the nuclear effects in DIS would be largely negligible because of the small nucleon binding energy compared to the high energies involved in DIS. However it was not confirmed by the experiment (known as EMC effect) (for review see e.g. [16]).

Starting from the middle of 80's there are many theoretical attempts to explain the EMC effect. In fact these models are phenomenological with some free parameter, based on a particular physical scenario assumed. The free parameters are fixed in order to reproduce the experimental data. The models can be generally divided in two groups:

- “conventional” nuclear physics models assuming either pions ($\approx 12\%$) and Δ ($\approx 4\%$) contributions to the nucleon structure function or using binding energy (x -rescaling) as free parameter or both. However, the binding energy needed to explain the experiment is however 3 to 4 times higher than the typical experimental values. Using the correct normalization of the spectral function and also the experimental separation energy, Li, Lui and Brown [17] estimated the contribution of the binding energy effects to account up to about 20% of observed depletion.

— QCD inspired picture - Q^2 -rescaling models assuming a change of the confinement size due to nucleon swelling. Typical values of swelling used are between 5% and 15%.

The chiral quark soliton model suggests a physical picture which includes the main features of both types of model:

- the contribution from the polarized Dirac sea with a non-vanishing quark condensate can be interpreted similar to the pion contribution. However, one should remember that pion loops are not considered;
- including of Δ excitation is possible but it is a diagram of the next order;
- the nucleon mass is getting reduced in medium (leads to a x -scaling);
- a swelling of 17% is predicted (leads to a Q^2 -scaling).

5 Conclusion

According to the chiral quark-soliton model the nucleon in baryon medium is getting swelled and its mass is reduced as well. Both the nucleon electric and magnetic coupling constants and form factors are getting reduced in the baryon medium. The axial coupling constant g_A as well as the corresponding nucleon axial form factor are getting reduced in baryon medium which is the expected correct behavior. The coupling constant $g_{\pi NN}$ is almost not affected by medium but the corresponding form factor $G_{\pi NN}$ is showing a significant reduction at finite momentum transfers in the medium. Such a behavior should be taken into account in the construction of the NN potential (especially its isovector tensor part) for description of the N -nucleus scattering or in charge-exchange reactions. Using the medium-modified nucleon electric form factors within the CDFM the longitudinal response function is calculated for a variety of nuclei showing a remarkable good agreement with the experimental data. The medium modified nucleon properties are consistent with the parameter values used in different phenomenological models describing the EMC effect.

Acknowledgements

The author is grateful for the financial support of the Bulgarian Science Fund under Contract No. DFNIT02/19.

References

- [1] The Frontiers of Nuclear Science, A Long Range Plan (2008); <https://arxiv.org/abs/0809.3137>.
- [2] Y. Nambu and G. Jona-Lasinio, *Phys. Rev.* **122** (1961) 354.
- [3] S. Kahana, G. Ripka, *Nucl. Phys. A* **429** (1984) 462.
- [4] D.I. Diakonov, V. Petrov, *Nucl. Phys. B* **245** (1984) 249.
- [5] G. 'tHooft, *Nucl. Phys. B* **72** (1974) 461.
- [6] M. Gell-Mann and M. Levy, *Nuovo Cim.* **16** (1960) 705.

Are Medium Modifications of the Nucleon Structure Suggested by ...

- [7] Chr. V. Christov, A. Blotz, H.-C. Kim, PV. Pobylitsa, T. Watabe, Th. Meissner, E. Ruiz Arriola and K. Goeke, *Prog. Part. Nucl. Phys.* **37** (1996) 1.
- [8] J. Berger, Chr. V. Christov, *Nucl. Phys. A* **609** (1996) 537.
- [9] Chr. V. Christov, Proceedings of the 37-th International Workshop on Nuclear Theory, Rila Mountains, 2018, NUCLEAR THEORY, Vol. 37 (2018), ISSN 1313-2822, 211.
- [10] Chr. V. Christov, E. Ruiz Arriola and K. Goeke, Lecture at XXX Cracow School of Theoretical Physics. June 2-12, 1990, Zakopane, Poland, *Acta Phys. Polonica* **22** (1991) 187.
- [11] Chr. V. Christov, E. Ruiz Arriola and K. Goeke, *Nucl. Phys. A* **510** (1990) 689.
- [12] Chr. V. Christov and K. Goeke, *Nucl. Phys. A* **564** (1993) 551.
- [13] G. Höhler et al., *Nucl. Phys. B* **114** (1976) 505.
- [14] A. Del Guerra et al., *Nucl. Phys. B* **114** (1976) 65.
- [15] A.N. Antonov, V.A. Nikolaev, and I.Zh. Petkov, *Z. Phys. A* **297** (1980) 151; *Z. Phys. A* **304** (1994) 239; A.N. Antonov, D.N. Kadrev, and P.E. Hodgson, *Phys. Phys. C* **50** (1994) 164.
- [16] Z.E. Meziani et al., *Phys. Rev. Lett.* **52** (1984) 2130; P. Batteau et al., *Nucl. Phys. A* **402** (1983) 515; Z.E. Meziani et al., *Phys. Rev. Lett.* **54** (1985) 1233; C.C. Blatchley et al., *Phys. Rev. C* **34** (1986) 1243; A. Zghiche et al., in Proc. PANIC XII (MIT, Cambridge, MA, 1990) I-8a.
- [17] M. Arneodo, *Phys. Rep.* **240** (1994) 304.
- [18] G.L. Li, K.F. Liu and G.E. Brown, *Phys. Lett. B* **213** (1988) 513.